


Synthesis of aryldifluoromethyl aryl ethers via nickel-catalyzed suzuki cross-coupling between aryloxydifluoromethyl bromides and boronic acids

Heng Lu^{1,2}, Ruo-Xuan Xiao^{1,2}, Chang-Yun Shi¹, Zi-Lan Song¹, Hou-Wen Lin¹ & Ao Zhang ¹✉

As a unique organofluorine fragment, gem-difluoromethylated motifs have received widespread attention. Here, a convenient and efficient synthesis of aryldifluoromethyl aryl ethers (ArCF₂OAr') was established via Nickel-catalyzed aryloxydifluoromethylation with aryl-boronic acids. This approach features easily accessible starting materials, good tolerance of functionalities, and mild reaction conditions. Diverse late-stage difluoromethylation of many pharmaceuticals and natural products were readily realized. Notably, a new difluoromethylated PD-1/PD-L1 immune checkpoint inhibitor was conveniently synthesized and showed both improved metabolic stability and enhanced antitumor efficacy. Preliminary mechanistic studies suggested the involvement of a Ni(I/III) catalytic cycle.

¹Pharm-X Center, College of Pharmaceutical Sciences, Shanghai Jiao Tong University, 800 Dongchuan Road, Shanghai 200240, China. ²These authors contributed equally: Heng Lu, Ruo-Xuan Xiao. ✉email: ao6919zhang@sjtu.edu.cn

In recent decades, fluorine-containing molecules have gained tremendous importance in the field of drug discovery, approximately accounting for over 30% of the total and crossing diverse disease indications^{1–4}. Among these, *gem*-difluoromethylated ones are a unique class of organofluoro compounds, due to the capability of difluoromethyl motif both in creating new patentable intellectual property and in improving druglike properties, such as metabolically masking of carbonyl, bioisosteric replacement of methylene, amide, ether and esters^{5,6}. More specifically, the aryldifluoromethyl aryl ether module ($\text{ArCF}_2\text{OAr}'$) has attracted increasing interests recently due to its optimal metabolic stability against benzylic oxidation by CYP450 enzyme in liver and similar or slightly improved biological activity, compared to the non-fluorinated precursors $\text{ArCH}_2\text{OAr}'$ ^{7–12}. A few representative druglike compounds bearing $\text{ArCF}_2\text{OAr}'$ structural scaffold are listed in Fig. 1, including antitumor kinase inhibitors I and II^{7,8}, antimalarial compound III⁹, guanylate cyclase activator IV¹⁰, antiviral compound V¹¹, and PD-1/PD-L1 interaction inhibitor VI¹².

Compared to alkyl difluoromethyl aryl/alkyl ethers, approaches to access aryldifluoromethyl aryl ethers are limited. Early in 1990¹³, Zupan and coworkers demonstrated a XeF_2 -introduced fluorination-rearrangement reaction of diarylketones under strong acidic condition, leading to aryldifluoromethyl aryl ethers (Fig. 1b-a). Later, Sekiya¹⁴ and Hitchcock¹⁵ respectively reported some modifications of this strategy by using various moderate acids. However, this strategy was restricted by the use of tedious XeF_2 as fluorination agent and suffered from narrow substrate compatibility. The classical oxidative desulfurization-difluorination of esters using Lawson's reagent or alkyl dithiols is also an option of choices to prepare aryldifluoromethyl aryl ethers (Fig. 1b-b). This method also suffers from several disadvantages, such as using smelly reagents and unstable

fluorination reagents^{16–18}. Direct nucleophilic substitution of aromatic *gem*-difluoromethyl halides or its equivalents by phenols has been reported to deliver aryldifluoromethyl aryl ethers readily (Fig. 1b-c-I)^{19–21}. As an improvement, Hu's group recently presented a radical nucleophilic substitution strategy of fluoroalkyl sulfones substituted phenanthridines by phenolates to build $\text{ArCF}_2\text{OAr}'$ module through a single-electron transfer (SET) process (Fig. 1b-c-II)²². Shortly thereafter, Young's group^{23,24} developed a frustrated Lewis-pair-mediated C-F activation of trifluoromethylarenes with 2,4,6-triphenylpyridine (TPPy) leading to active ArCF_2 -TPPy salts, which then underwent substitution with suitable lithium aryloxides to afford aryl aryloxydifluoromethyl ethers (Fig. 1b-c-III). Unfortunately, these nucleophilic substitution strategies suffer from harsh reaction conditions and limited substrate scopes. Recently, Qing and co-workers²⁵ developed a direct C-H aryloxydifluoromethylation of heteroarenes through Ag-catalyzed decarboxylation of aryloxydifluoroacetic acids to afford $\text{ArCF}_2\text{OAr}'$ species (Fig. 1b-d-I). However, this approach is limited to heteroaryl compounds.

Despite these available approaches to access $\text{ArCF}_2\text{OAr}'$, they are generally limited to harsh reaction conditions, complex fluorine agents, and narrow substrate scopes. Therefore, developing a mild, highly substrate compatible, and site-selective method for convenient construction of $\text{ArCF}_2\text{OAr}'$ remains highly desirable. Inspired by the wide use of mono- or difluoromethyl halides in the transition-metal catalyzed C-C coupling reactions with different partners^{26–37}, herein, we reported a Ni-catalyzed Suzuki cross-coupling reaction by using aryloxydifluoromethyl bromides (ArOCF_2Br) as a unique halide species to undergo coupling with arylboronic acids, leading to highly efficient synthesis of various aryl aryloxydifluoromethyl ethers (Fig. 1b-d-II).

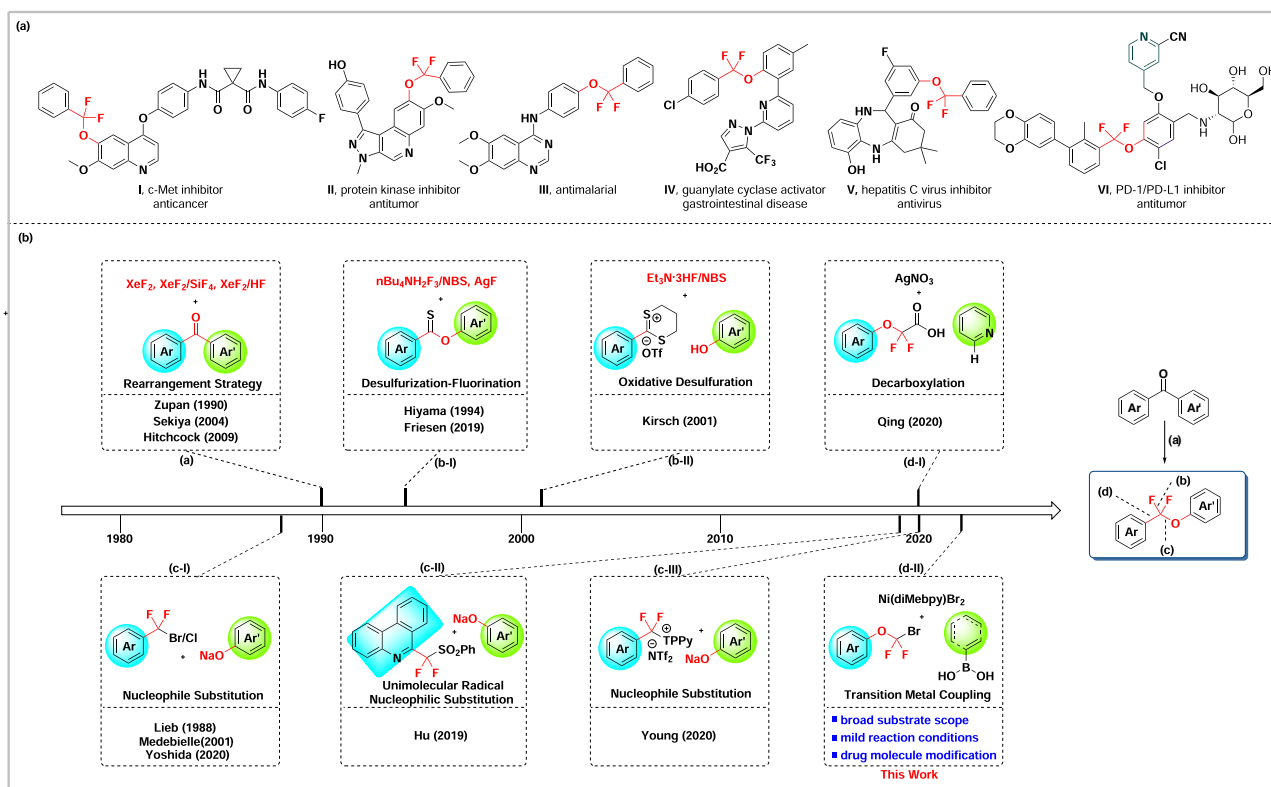
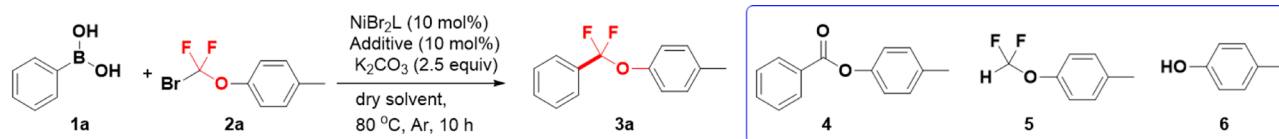
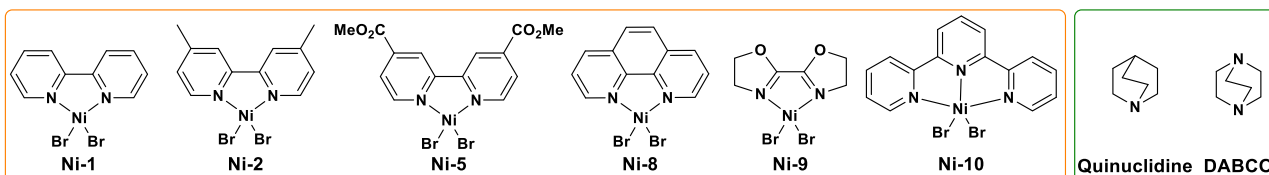


Fig. 1 Overview of methods to prepare aryl aryloxydifluoromethyl ethers. **a** Examples of biologically active aryl aryloxydifluoromethyl ethers. **b** Synthetic methods for aryl aryloxydifluoromethyl ethers.

Table 1 Reaction optimization^a.

Entry	NiBr ₂ L (10 mmol%)	Solvent	Additive (10 mmol %)	Yield ^b (3a/4/5, %)
1	Ni-1	DMF	-	21/15/27
2	Ni-1	NMP	-	N.D./N.D./N.D.
3	Ni-1	DMSO	-	N.D./N.D./N.D.
4	Ni-1	dioxane	-	N.D./N.D./37
5	Ni-1	acetone	-	40/16/N.D.
6	Ni-1	EA	-	36/33/15
7	Ni-1	MeCN	-	32/19/11
8 ^c	Ni-1	acetone	-	45/10/N.D.
9 ^d	Ni-1	acetone	-	N.D./5/14
10 ^c	Ni-2	acetone	-	55/15/N.D.
11 ^c	Ni-5	acetone	-	38/21/N.D.
12 ^c	Ni-8	acetone	-	32/17/18
13 ^c	Ni-9	acetone	-	N.D./N.D./11
14 ^c	Ni-10	acetone	-	N.D./N.D./15
15 ^c	Ni-2	acetone	Py	67/12/5
16 ^c	Ni-2	acetone	PPh ₃	59/10/21
17 ^c	Ni-2	acetone	NPh ₃	60/13/11
18 ^c	Ni-2	acetone	quinuclidine	82/6/N.D.
19 ^c	Ni-2	acetone	DABCO	90(86) ^e /6/N.D.
20 ^c	-	acetone	DABCO	N.D./N.D./N.D.



^aReaction condition: **1a** (0.4 mmol), **2a** (0.2 mmol), NiBr₂L (10 mol%), additive (10 mol%), K₂CO₃ (0.5 mmol), solvent (3 mL), 80 °C, 10 h.

^bYields were determined by GC-MS with *n*-dodecan as an internal standard.

^cUsing dry acetone as solvent.

^dOne drop of water was added.

^eIsolated yield.

Results and discussion

Optimization studies. Firstly, we used phenylboronic acid (**1a**) and (4-tolyloxy)difluoromethyl bromide (**2a**) as the model substrates, (2,2'-bipyridine)nickel(II) dibromide (Ni-1) as the catalyst, K₂CO₃ as the base and DMF as the solvent (for details see Table S1–Table S7 in SI). The expected product **3a** was obtained in 21% yield, along with oxodefluorinated **4** (15%)^{38–40}, hydrodebrominated **5** (27%)^{41–44} and phenol (**6**, trace) as byproducts (Table 1, entry 1). Then, we tested different solvents to reduce the oxygendifluorination liability (entries 1–8) and acetone was found as a more appropriate solvent to afford product **3a** in 40% yield and byproducts **4** and **5** were much suppressed (entry 5). with the participation of water, **4** may result from Ni-CF₂OAr complex via oxidative defluorination or from the hydrolysis of product **3**. The yield of **3a** was further improved to 45% when dry acetone was used (Table 1, entry 8). As a contrast, adding water (one drop) to the reaction led to no detectable product (entry 9). Next, various Ni-containing catalysts were examined (entries 10–14). The Ni complex Ni-2 bearing an electronic-rich ligand showed higher efficiency than phen-Ni complex and other diamine or triamine bonding Ni complexes, providing **3a** in 55% yield (entry 10). Further, an additive was added to modulate the electronic and

steric properties of the nickel center to facilitate the catalytic cycle^{30–32}. Among the different nitrogen and phosphorus ligands tested, electron-donating alkylamines were found more effective than pyridine derivatives, arylamines, and phosphorus ligands. The best result was obtained using DABCO as the ligand, providing the expected product **3a** in 90% yield (entry 19). Ni-complexed catalyst was found necessary for this coupling (Table 1, entry 20).

Scope of the reaction. With the optimized reaction condition in hand (Table 1, entry 19), the scope of arylboronic acids was investigated. As shown in Fig. 2, various arylboronic acids bearing either electron-withdrawing or electron-donating substituents were successfully coupled with (4-tolyloxy)difluoromethyl bromide **2a** to deliver the corresponding aryloxydifluoromethylated products **3a–3z** in moderate to good yields. Arylboronic acids bearing a hydroxymethyl or cyano-substituent survived very well in this reaction and the corresponding products **3i** and **3o** were obtained in 75% and 55% yields, respectively, which provide potentials for further functional transformation. In certain cases, a mixed solvent of acetone/DMF was used to increase the

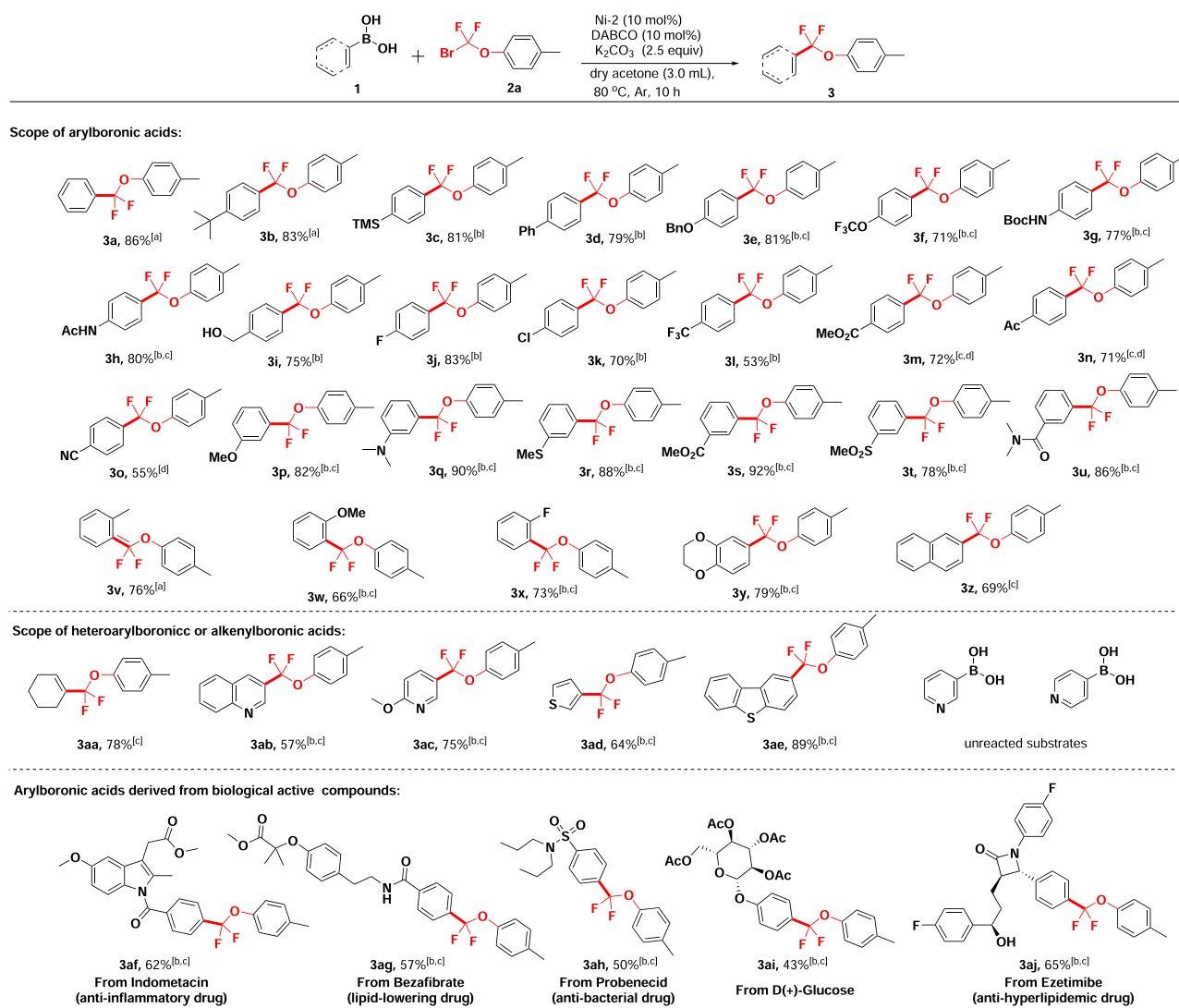


Fig. 2 Ni-catalyzed aryloxydifluoromethylation reactions with diversified arylboronic acids. **a** Reaction conditions: unless otherwise noted, a solution of **1** (0.2 mmol), **2a** (0.4 mmol), Ni-2 (10 mol%), DABCO (10 mol%), and K_2CO_3 (0.5 mmol) in dry acetone (3.0 mL) was performed at 80 °C under argon for 10 h. The yields are isolated yields by column chromatography on silica gel. **b** Dry acetone (2.5 mL) and DMF (0.5 mL) were used for solvent. **c** 100 mg 4 Å MS was added. **d** Dry acetone (1.5 mL) and DMF (1.5 mL) were used for solvent.

solubility of substrates and molecular sieves was added to suppress the defluorination liability of the products.

It is noted that arylboronic acids containing electron-donating functional groups at the *para*-position, such as methoxyl and methylthioyl, failed to give the expected difluorinated products, due to oxidative defluorination during purification by silica gel column chromatography. Slightly lower yields were obtained for arylboronic acids bearing ortho-substituents (**3v–3x**, 66–76%). Bicyclic and naphthyl boronic acids were found suitable as well to provide the corresponding products **3y** and **3z** in 79% and 69% yields, respectively. Meanwhile, cyclohex-1-en-1-ylboronic acid also successfully participated in this coupling reaction and provided the product **3aa** in 78% yield. To our delight, quinolinyl, pyridinyl, thiophenyl and dibenzothiophenyl boronic acids underwent the reaction smoothly as well leading to corresponding products **3ab–3ae** in 57–89% yields. We have also tried unsubstituted pyridineboronic acids as substrates, and we failed to detect any corresponding products. More practically, this Ni-catalyzed reaction was also applied to arylboronic acids derived from biologically active compounds (including anti-inflammatory, anti-

bacterial, anti-hyperlipidemic drugs and glucose) and the corresponding products **3af–3aj** were readily obtained in moderate to good yields.

To further explore the substrate scope, various aryloxydifluoromethyl bromides were explored to cross-couple with arylboronic acids. As shown in Fig. 3, aryloxydifluoromethyl bromides bearing different substituents on the aryl including methoxy (**7a**), methyl (**7c**), and chloro (**7d**, **7g**) readily went through the coupling reactions with arylboronic acid and afforded corresponding products in high yields. Biphenyloxydifluoromethyl bromide bearing a hydroxymethyl substituent was also a suitable substrate for coupling with arylboronic acids yielding compounds **7e** and **7h** in 71% and 56% yields, respectively, which can be used for further transformation. Bicyclic aryloxydifluoromethyl bromides smoothly participated in the reaction as well giving compounds **7b** and **7f** in 71% and 57% yields, respectively. Notably, cross-coupling of arylthiodifluoromethyl bromides with arylboronic acids also occurred smoothly to deliver the corresponding difluoromethylated species **7i** and **7j** in 53% and 40% yields, respectively (Fig. 3).

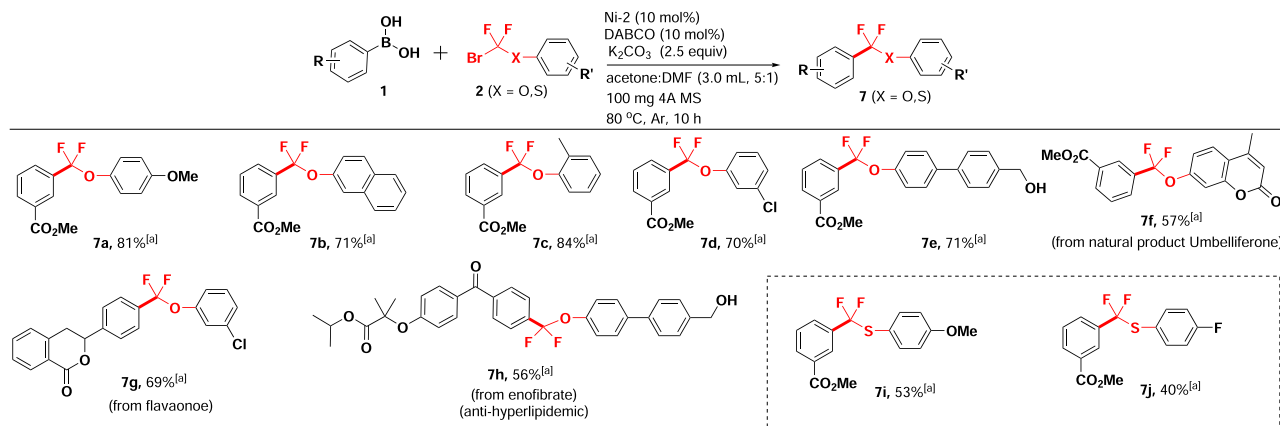


Fig. 3 Ni-catalyzed aryloxydifluoromethylation reactions with various difluoromethyl bromides. a Reaction conditions: unless otherwise noted, a solution of **1** (0.2 mmol), **2** (0.4 mmol), Ni-2 (10 mol%), DABCO (10 mol%), 100 mg 4 A MS and K_2CO_3 (0.5 mmol) in dry acetone (2.5 mL) and DMF (0.5 mL) was performed at 80 °C under argon for 10 h. The yields are isolated yields.

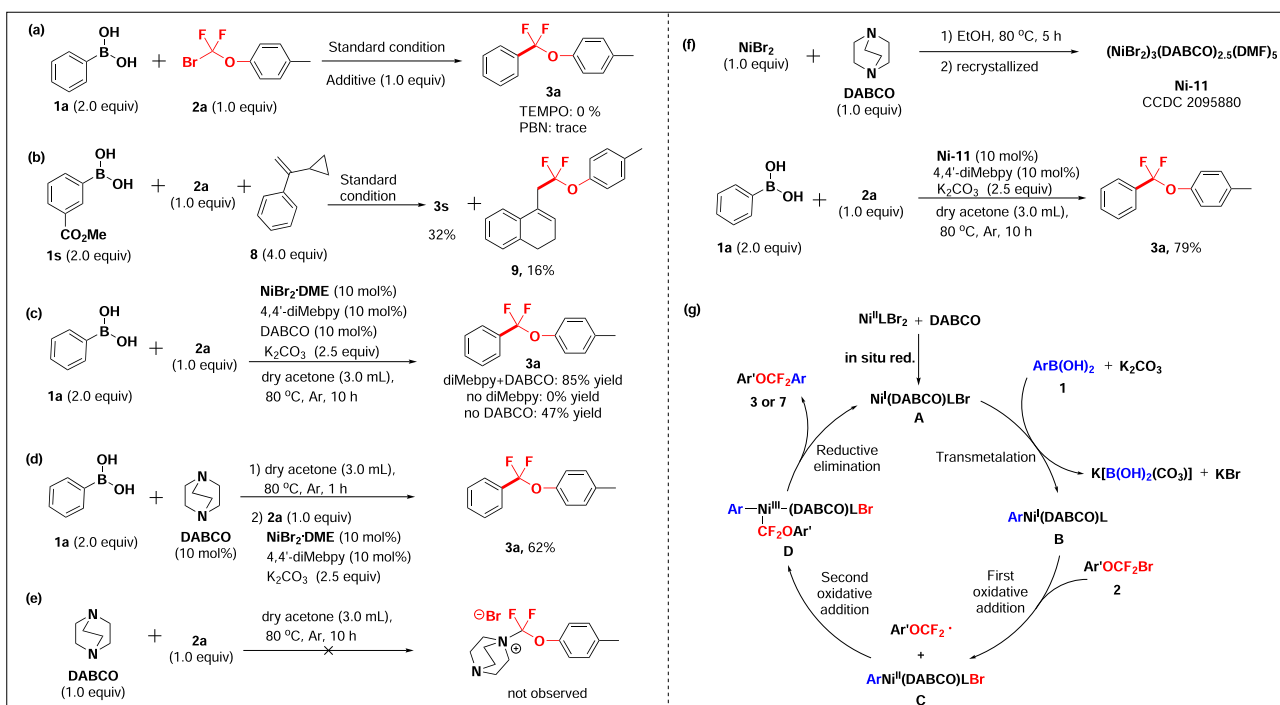


Fig. 4 Mechanistic studies and proposed mechanism. a Radical inhibition experiments. **b** Radical clock experiments. **c** The reaction proceeds under $NiBr_2 \cdot DME$, 4,4'-diMeby and DABCO. **d** The reaction proceeds through pretreatment of DABCO and phenylboronic acid **1a**. **e** Salt-forming experiment between DABCO and aryloxydifluoromethyl bromides **2a**. **f** The reaction proceeds under Ni(II) complexes $[(NiBr_2)_3(DABCO)_{2.5}(DMF)_5]$ and 4,4'-diMeby. **g** Proposed catalytic cycles.

Mechanistic investigations. To verify the reaction mechanism, several investigational experiments were conducted (Fig. 4). First, we found that the model reaction of **1a** and **2a** did not occur when the radical trapping reagent TEMPO (1.0 equiv) or *N*-tert-butyl- α -phenylnitron (PBN, 1.0 equiv) was applied (Fig. 4a). Meanwhile, when the single electron transfer inhibitor 1,4-dinitrobenzene was added, the reaction was also blocked, indicating that a single-electron transfer of radicals was involved in this reaction (for details see SI, page S48). Moreover, a radical trapping product **9** (16% yield) was obtained when α -cyclopropyl styrene **8** was added in the reaction of **1s** and **2a** under standard condition (Fig. 4b).

In order to explore whether DABCO (1,4-diaza[2.2.2]bicyclooctane) acted as a co-ligand to coordinate with the nickel

complex to promote the reaction, we conducted a few additional experiments. Firstly, the catalyst $NiBr_2 \cdot DME$, 4,4'-diMeby and DABCO were added to the reaction of **1a** and **2a** under the standard condition (Fig. 4c). Product **3a** was detected in 85% yield, which was nearly identical to the result obtained under optimum condition (90% yield). On the other hand, in the absence of DABCO, the yield of product was drastically reduced (55%); however, in the absence of the bipyridine ligand, the reaction failed to take place, which indicates that bipyridine ligand is an essential request and DABCO has a strong role in facilitating the reaction. Further, pretreating DABCO with phenylboronic acid **1a** in acetone at 80 °C for 1 h, followed by addition of substrate **2a**, $NiBr_2 \cdot DME$, 4,4'-diMeby and K_2CO_3 led to product **3a** in much reduced yield (62%, Fig. 4d). This result

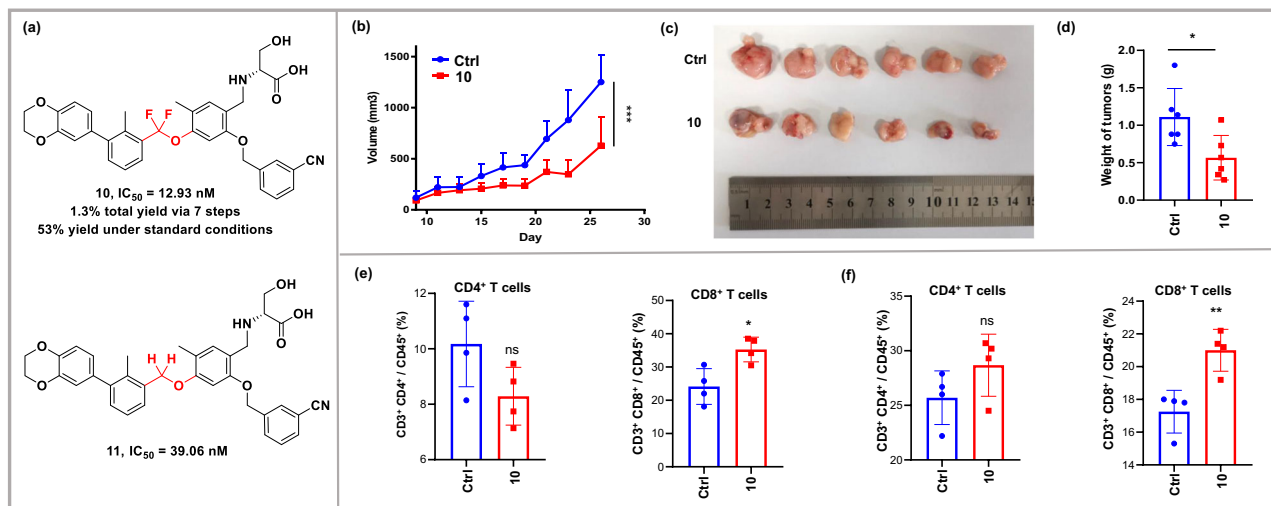


Fig. 5 Treatment with compound 10 inhibited tumor growth in vivo and remodeled facilitated the infiltration of CD8⁺ T cells. **a** PD-1/PD-L1 immune checkpoint inhibitor activity of difluorinated compound 10 and non-fluoro compound 11. **b** The growth of transplanted MC38 tumors after local injection of 20 mg/kg compound 10 or vehicle daily. Data are presented as mean \pm SEM ($n = 8$, *** $P < 0.001$, two-way ANOVA). **c** Image of excised tumors from. **d** weight of excised tumors from. **e** Representative plots (left) and frequency (right) of CD4⁺ T cells and CD8⁺ T cells in tumors. **f** Representative plots (left) and frequency (right) of CD4⁺ T cells and CD8⁺ T cells in spleens, data are presented as mean \pm SD ($n = 4$, ns $P > 0.05$, * $P < 0.05$, ** $P < 0.01$, *t* test).

suggests that DABCO has no activating effect on the arylboronic acid. In addition, to exclude the possible activation of difluoromethyl bromide 2a via DABCO to give an active electrophilic species as a reaction precursor, we treated these two species equivalently for 10 h at 80 °C, and no reaction precursor (a quaternary ammonium salt) was detected (analyzed by ¹⁹F NMR) (Fig. 4e). Finally, we synthesized nickel-DABCO complex [(NiBr₂)₃(DABCO)_{2.5}(DMF)₅] (Ni-11), which was characterized through X-ray single crystal diffraction (for details see Fig. S1 and Table S8 in SI). Compound 3a was achieved in a comparable yield of 79% when phenylboronic acid 1a was reacted with 2a in the presence of the complex Ni-11 and the challenging ligand 4,4'-diMeby (Fig. 4f). Together, all these experiments confirm that DABCO plays as a co-ligand to coordinate with the nickel catalyst and facilitates the catalytic cycle.

Proposed mechanism. Based on our experimental results and literature reports^{45–50}, we envisioned a tentative mechanism involving a Ni(I/III) catalytic cycle. As shown in Fig. 4g, a nickel (I) complex [Ni(I)(DABCO)LBr] (A) might be formed first in situ reduction of nickel (II) species through boronic acid, which then undergoes a transmetalation process with arylboronic acid 1 and K₂CO₃ to form arylnickel complex [ArNi(I)(DABCO)L] (B). Subsequent reaction with aryloxydifluoromethyl bromide 2 occurs likely through a single electron transfer pathway to produce the arylnickel(aryloxydifluoromethyl) complex [ArNi(II)(DABCO)LBr] (C) and aryloxydifluoromethyl radical. Further oxidative addition of aryloxydifluoromethyl radical to the complex C generates the key intermediate D. Finally, products 3 or 7 are obtained from a reductive elimination of the Ni(III) species D, along with regeneration of Ni(I) species A to complete the catalytic cycle.

Difluoromethylated PD-1/PD-L1 immune checkpoint inhibitor. To further confirm the practicability of the new Ni-catalyzed cross-coupling protocol, we applied this method to successfully prepare a new difluoromethylated PD-1/PD-L1 checkpoint inhibitor 10 in 1.3% total yield via 7 steps (for details see SI, page S39–S47). Diaryldifluoromethyl ether intermediate was obtained in 53% yield under standard conditions, which was difficult to prepare

using traditional oxidative desulfurization-difluorination method in our previous report (less than 10% yield)¹². As shown in Fig. 5a, compared to the non-fluoro precedent 11, difluorinated 10 showed three-fold higher potency against PD-1/PD-L1 interaction (IC_{50} for 10/11: 12.93 vs 39.06 nM). In vivo, inhibitor 10 displayed a significant reduction in tumor burden than control group with no significant loss of body weight or other common toxic effects in MC38 subcutaneous transplanted tumor model (Fig. 5b, c, d). Furthermore, to explore the effect of 10 on tumor immunity, we measured the percentage of T lymphocytes in tumors and spleens of mice treated with 10. As shown in Figs. 5e, f (for details see Fig. S2 in SI), injection of 10 significantly increased the population of CD8⁺ T cells in both tumors and spleens, which indicated that 10 activated antitumor immune response in MC38 xenograft model.

Conclusion

In summary, we have established an efficient strategy for the synthesis of a unique class of aryldifluoromethyl aryl ethers via Nickel-catalyzed cross-coupling of aryldifluoromethoxy bromides with arylboronic acids. The reaction showed wide substrate scope in both substrates containing various functional groups, and allowed late-stage difluoromethylation of many pharmaceuticals and natural products. Mechanistic studies revealed that this reaction might go through a Ni(I/III) catalytic cycle. Attractively, this method was successfully applied to readily synthesize a difluorinated PD-1/PD-L1 immune checkpoint inhibitor which showed much improved antitumor efficacy both in biochemical assay and in in vivo mice model. Therefore, this new protocol would provide ample potentials in the drug design and discovery filed.

Methods

Supplementary Methods. For more details, see Supplementary Information page S1.

General procedure for the synthesis of compound 3. To a dried 10 ml Schlenk-type tube equipped with a magnetic stir bar was charged with arylboronic acid 1a (49.0 mg, 0.4 mmol, 2.0 equiv), Ni-2 (8.0 mg, 0.02 mmol, 10 mol %), DABCO (2.3 mg, 0.02 mmol, 10 mol %) and K₂CO₃ (69.0 mg, 0.5 mmol, 2.5 equiv) under air. The reaction mixture was then evacuated and backfilled with Ar (3 times). 1-(bromodifluoromethoxy)-4-methylbenzene 2a (47.0 mg, 0.2 mmol, 1.0 equiv), and

acetone (3 mL) were added. The mixture was stirred at 80 °C for 10 h. After cooled to room temperature, the reaction mixture was filtered and the filtrate was concentrated. The residue was purified on a preparative TLC with petroleum ether/ethyl acetate as the eluent to afford the products **3a**.

General procedure for the synthesis of compound 7. To a dried 10 mL Schlenk-type tube equipped with a magnetic stir bar was charged with arylboronic acid **1** (72.0 mg, 0.4 mmol, 2.0 equiv), Ni-2 (8.0 mg, 0.02 mmol, 10 mol %), DABCO (2.3 mg, 0.02 mmol, 10 mol %), 100 mg 4 Å MS and K₂CO₃ (69.0 mg, 0.5 mmol, 2.5 equiv) under air. The reaction mixture was then evacuated and backfilled with Ar (3 times). 1-(bromodifluoromethoxy)-4-methoxybenzene **2b** (50.4 mg, 0.2 mmol, 1.0 equiv), and acetone (2.5 mL) and DMF (0.5 mL) were added. The mixture was stirred at 80 °C for 10 h. After cooled to room temperature, the reaction mixture was filtered and the filtrate was concentrated. The residue was purified on a preparative TLC with petroleum ether/ethyl acetate as the eluent to afford the products **7a**.

General procedure for the synthesis of metal-complex Ni-11. To a stirring solution of DABCO (336 mg, 3.0 mmol, 1.0 equiv) in EtOH (30 mL) was added NiBr₂ (648 mg, 3.0 mmol, 1.0 equiv), the reaction mixture was stirred at 80 °C for another 5 h, then the solution was filtrated and the filtrate was which was recrystallized from DMF and ^tBuOMe to give an orange solid.

Compound characterization. For more details, see Supplementary Data 1.

In vivo effect of compound 10. 6-week-old female mice were purchased from Shanghai SLAC Laboratory Animal Co., Ltd. The animal experimental protocols were approved by the Instructional Animal Care and Use Committee of Shanghai Jiao Tong University. 1 × 10⁶ MC38 cells were suspended in PBS and subcutaneously injected into the right axilla region of the mice. The volume of tumors were measured with vernier caliper and calculated using the formula: volume (mm³) = 0.5 × longest diameter × shortest diameter. When tumor volumes reached 100 mm³ (Day9), the mice were randomly divided into two groups, and subcutaneously injected with control solvent (5% DMSO, 55% PEG400, 40% H₂O) or compound **10** (20 mg/kg) around the tumor daily. Tumor volumes and body weight of mice were measured every two days. After 18 days, mice were sacrificed and the tumors were collected and weighted, and the spleens were collected simultaneously.

Immune cells infiltration in tumors and spleens. Tumor tissues were minced and digested in 1 mg/mL hyaluronidase, 1 mg/mL collagenase IV and 0.15 mg/mL DNase I for 2 hours and filtered with 70 μm strainer. Mononuclear cells were isolated with Ficoll-Paque PREMIUM 1.073 (Cytiva) as the manufacturer's instruction, and blocked with Purified Rat Anti-Mouse CD16/CD32 (BD Pharmingen) for 1 hours at 4 °C. After staining with Fixable Viability Stain 520, anti-mouse CD3e PerCP-Cy5.5, anti-mouse CD8a APC and anti-mouse CD4 PE (BD Pharmingen) for 30 min at 4 °C, the cells were washed and analyzed by a CytoFLEX flow cytometry (BECKMAN COULTER). The spleens were grinded and filtered with 70 μm strainer, followed by lysing red blood cell using BD Pharm Lyse™ lysing solution. The spleen cells were collected, blocked, stained and analyzed as described above. The data were analyzed by FlowJo 10.6.2.

Reporting summary. Further information on research design is available in the Nature Research Reporting Summary linked to this article.

Data availability

All the relevant data of this study are available within this paper and its Supplementary Information are available from the corresponding author upon reasonable request. This includes Supplementary Data 1, which includes all NMR spectra. In addition, the X-ray crystallographic data for Ni-11 are included in Supplementary Data 2 and Supplementary Data 3. Crystallographic data could be obtained free of charge from The Cambridge Crystallographic Data Center with the accession code CCDC 2095880 via www.ccdc.cam.ac.uk/data_request/cif.

Received: 27 April 2022; Accepted: 22 June 2022;

Published online: 04 July 2022

References

1. Myers, G., Barbay, J. K. & Zhong, B. Asymmetric synthesis of chiral organofluorine compounds: use of nonracemic fluorioiodoacetic acid as a practical electrophile and its application to the synthesis of monofluoro

- hydroxyethylene dipeptide isosteres within a novel series of HIV protease inhibitors. *J. Am. Chem. Soc.* **123**, 7207–7219 (2001).
2. Burke, T. R. & Lee, J. R. K. Phosphotyrosyl mimetics in the development of signal transduction inhibitors. *Acc. Chem. Res.* **36**, 426–433 (2003).
3. Romanenko, V. D. & Kukhar, V. P. Fluorinated phosphonates: synthesis and biomedical application. *Chem. Rev.* **106**, 3868–3935 (2006).
4. Purser, S., Moore, P. R., Swallow, S. & Gouverneur, V. Fluorine in medicinal chemistry. *Chem. Soc. Rev.* **37**, 320–330 (2008).
5. Müller, K., Faeh, C. & Diederich, F. Fluorine in pharmaceuticals: looking beyond intuition. *Science* **317**, 1881–1886 (2007).
6. Wang, J., Sorochinsky, A. E., Fustero, S., Soloshonok, V. A. & Liu, H. Fluorine in pharmaceutical industry: fluorine-containing drugs introduced to the market in the last decade (2001–2011). *Chem. Rev.* **114**, 2432–2506 (2014).
7. Lien, V. T. et al. Design, synthesis and biological evaluation of 6-substituted quinolines derived from cabozantinib as c-Met inhibitors. *Arch. Pharm. Chem. Life Sci.* **352**, 1900101 (2019).
8. Thomas, F., Werner, M. & Frank, Z. Pyrazoloquinolines as serine-threonine protein kinase inhibitors and their preparation and use in the treatment of cancer. WO 2012000632 A1 (2012).
9. Gamo, F. J. et al. Thousands of chemical starting points for antimalarial lead identification. *Nature* **465**, 305–310 (2010).
10. Bittner, A. R. et al. Preparation of propanoic acid derivatives for treatment of diabetes. WO 2009032249 A1 (2009).
11. Pierre, J. M., Origene, N., Katie, I. E., Hu, L.-L. & Carlo, W. M. 6-Hydroxydibenzodiazepinones useful as hepatitis C virus inhibitors and their preparation and use in the treatment of hepatitis C. WO 2008099019 A1 (2008).
12. Song, Z.-L. et al. Design, synthesis, and pharmacological evaluation of biaryl-containing PD-1/PD-L1 interaction inhibitors bearing a unique difluoromethyleneoxy linkage. *J. Med. Chem.* **64**, 16687–16702 (2021).
13. Zajc, B. & Zupan, M. Fluorination with xenon difluoride. 37. room-temperature rearrangement of aryl-substituted ketones to difluoro-substituted ethers. *J. Org. Chem.* **55**, 1099–1102 (1990).
14. Tamura, M., Matsukawa, Y., Quan, H.-D., Mizukado, J. & Sekiya, A. Reaction of carbonyl compounds with xenon difluoride in the presence of silicon tetrafluoride. *J. Fluor. Chem.* **125**, 705–709 (2004).
15. Bartberger, M. D. et al. Synthesis and conformational analysis of α,α-difluoroalkyl heteroaryl ethers. *Tetrahedron Lett.* **50**, 5452–5455 (2009).
16. Kuroboshi, M. & Hiyama, T. A facile synthesis of α,α-difluoroalkyl ethers and carbonyl fluoride acetals by oxidative desulfurization-fluorination. *Synlett.* **4**, 251–252 (1994).
17. Bremer, M., Taugerbeck, A., Wallmichrath, T. & Kirsch, P. Difluoroxyethylene-bridged liquid crystals: a novel synthesis based on the oxidative alkoxydifluorodesulfuration of dithianylum salts. *Angew. Chem. Int. Ed.* **40**, 1480–1484 (2001).
18. Newton, J. et al. A convenient synthesis of difluoroalkyl ethers from thionoesters using silver(I) fluoride. *Chem. Eur. J.* **25**, 15993–15997 (2019).
19. Haas, A., Spitzer, M. & Lieb, M. Synthese seitenkettenfluorierter aromatischer Verbindungen und deren chemische reaktivität. *Chem. Ber.* **121**, 1329–1340 (1988).
20. Burkholder, C. R., Dolbier, W. R. Jr & Médebielle, M. Synthesis and reactivity of halogeno-difluoromethyl aromatics and heterocycles: Application to the synthesis of gem-difluorinated bioactive compounds. *J. Fluor. Chem.* **109**, 39–48 (2001).
21. Idogawa, R., Kim, Y., Shimomori, K., Hosoya, T. & Yoshida, S. Single C–F transformations of *o*-hydrosilyl benzotrifluorides with trityl compounds as all-in-one reagents. *Org. Lett.* **22**, 9292–9297 (2020).
22. Xiao, P. et al. Fluoroalkylation of various nucleophiles with fluoroalkyl sulfones through a single electron transfer process. *J. Org. Chem.* **84**, 8345–8359 (2019).
23. Mandal, D., Gupta, R., Jaiswal, A. K. & Young, R. D. Frustrated Lewis-pair-mediated selective single fluoride substitution in trifluoromethyl groups. *J. Am. Chem. Soc.* **142**, 2572–2578 (2020).
24. Kim, Y., Kanemoto, K., Shimomori, K., Hosoya, T. & Yoshida, S. Functionalization of a single C–F bond of trifluoromethylarenes assisted by an ortho-silyl group using a trityl-based all-in-one reagent with ytterbium triflate catalyst. *Chem. Eur. J.* **26**, 6136–6140 (2020).
25. Zhu, X.-L., Huang, Y., Xu, X.-H. & Qing, F.-L. Silver-catalyzed C–H aryloxydifluoromethylation and arylthiodifluoromethylation of heteroarenes. *Org. Lett.* **22**, 5451–5455 (2022).
26. Jiang, X., Sakthivel, S., Kulbitski, K., Nisnevich, G. & Gandelman, M. Efficient synthesis of secondary alkyl fluorides via Suzuki C–coupling reaction of 1-halo-1-fluoroalkanes. *J. Am. Chem. Soc.* **136**, 9548–9551 (2014).
27. Xiao, Y.-L., Guo, W.-H., He, G.-Z., Pan, Q. & Zhang, X. Nickel-catalyzed cross-coupling of functionalized difluoromethyl bromides and chlorides with aryl boronic acids: a general method for difluoroalkylated arenes. *Angew. Chem. Int. Ed.* **53**, 9909–9913 (2014).

28. Gu, J.-W., Guo, W.-H. & Zhang, X. Synthesis of diaryldifluoromethanes by Pd-catalyzed difluoroalkylation of arylboronic acids. *Org. Chem. Front.* **2**, 38–41 (2015).
29. Jiang, X.-J. & Gandelman, M. Enantioselective Suzuki cross-couplings of unactivated 1-fluoro-1-haloalkanes: synthesis of chiral β -, γ -, δ -, and ϵ -fluoroalkanes. *J. Am. Chem. Soc.* **137**, 2542–2547 (2015).
30. An, K., Xiao, Y.-L., Min, Q.-Q. & Zhang, X. Facile access to fluoromethylated arenes by nickel-catalyzed cross coupling between arylboronic acids and fluoromethyl bromide. *Angew. Chem. Int. Ed.* **54**, 9079–9083 (2015).
31. Xiao, Y.-L., Min, Q.-Q., Xu, C., Wang, R.-W. & Zhang, X. Nickel-catalyzed difluoroalkylation of (hetero)arylborons with unactivated 1-bromo-1,1-difluoroalkanes. *Angew. Chem. Int. Ed.* **55**, 5837–5841 (2016).
32. Xu, C., Guo, W.-H., He, X., Gou, Y.-L. & Zhang, X. Difluoromethylation of (hetero)aryl chlorides with chlorodifluoromethane catalyzed by nickel. *Nat. Commun.* **9**, 1170–1180 (2018).
33. Sheng, J., Ni, H.-Q., Liu, G., Li, Y. & Wang, X.-S. Combinatorial nickel-catalyzed monofluoroalkylation of aryl boronic acids with unactivated fluoroalkyl iodides. *Org. Lett.* **19**, 4480–4483 (2017).
34. Sap, J. B. I. et al. Synthesis of ^{18}F -difluoromethylarenes using aryl boronic acids, ethyl bromofluoroacetate and ^{18}F fluoride. *Chem. Sci.* **10**, 3237–3241 (2019).
35. Huang, W., Wan, X. & Shen, Q. Cobalt-catalyzed asymmetric cross-coupling reaction of fluorinated secondary benzyl bromides with lithium aryl boronates/ ZnBr_2 . *Org. Lett.* **22**, 4327–4332 (2020).
36. Gupta, R., Mandal, D., Jaiswal, A. K. & Young, R. D. FLP-catalyzed monoselective C–F functionalization in polyfluorocarbons at geminal or distal sites. *Org. Lett.* **23**, 1915–1920 (2021).
37. Luo, Y.-C., Tong, F.-F., Zhang, Y., He, C.-Y. & Zhang, X. Visible-light-induced palladium-catalyzed selective defluoroarylation of trifluoromethylarenes with arylboronic acids. *J. Am. Chem. Soc.* **143**, 13971–13979 (2021).
38. Xu, Z.-W., Xu, W.-Y., Pei, X.-J., Tang, F. & Feng, Y.-S. An efficient method for the N-formylation of amines under catalyst- and additive-free conditions. *Tetrahedron Lett.* **60**, 1254–1258 (2019).
39. Su, J., Ma, X., Ou, Z. & Song, Q. Deconstructive functionalizations of unstrained carbon-nitrogen cleavage enabled by difluorocarbene. *ACS. Cent. Sci.* **6**, 1819–1826 (2020).
40. Jiang, X. et al. Autocatalytic synthesis of thioesters via thiocarbonylation of gem-difluoroalkenes. *Org. Lett.* **22**, 9762–9766 (2020).
41. Weires, N. A., Baker, E. L. & Garg, N. K. Nickel-catalysed Suzuki-Miyaura coupling of amides. *Nat. Chem.* **8**, 75–79 (2016).
42. Huang, P.-Q. & Chen, H. Ni-Catalyzed cross-coupling reactions of N-acylpyrrole-type amides with organoboron reagents. *Chem. Commun.* **53**, 12584–12587 (2017).
43. Li, X.-F., Zhang, X.-G., Chen, F. & Zhang, X.-H. Copper-catalyzed N-formylation of amines through tandem amination/hydrolysis/decarboxylation reaction of ethyl bromodifluoroacetate. *J. Org. Chem.* **83**, 12815–12821 (2018).
44. Ma, X., Yu, X., Huang, H., Zhou, Y. & Song, Q. Synthesis of thiazoles and isothiazoles via three-component reaction of enaminoesters, sulfur, and bromodifluoroacetamides/esters. *Org. Lett.* **22**, 5284–5288 (2020).
45. Ma, X. & Song, Q. Recent progress on selective deconstructive modes of halodifluoromethyl and trifluoromethyl-containing reagents. *Chem. Soc. Rev.* **49**, 9197–9219 (2020).
46. Jones, G. D. et al. Ligand redox effects in the synthesis, electronic structure, and reactivity of an alkyl-alkyl cross-coupling catalyst. *J. Am. Chem. Soc.* **128**, 13175–13183 (2006).
47. Lin, X. & Phillips, D. L. Density functional theory studies of Negishi alkyl-alkyl cross-coupling reactions catalyzed by a methylterpyridyl-Ni(I) complex. *J. Org. Chem.* **73**, 3680–3688 (2008).
48. Wilsily, A., Tramutola, F. N., Owston, A. & Fu, G. C. New directing groups for metal-catalyzed asymmetric carbon–carbon bond-forming processes: stereoconvergent alkyl-alkyl Suzuki cross-couplings of unactivated electrophiles. *J. Am. Chem. Soc.* **134**, 5794–5797 (2012).
49. Zultanski, S. L. & Fu, G. C. Nickel-catalyzed carbon-carbon bond-forming reactions of unactivated tertiary alkyl halides: Suzuki arylations. *J. Am. Chem. Soc.* **135**, 624–627 (2013).
50. Cornella, J., Gomez-Bengoa, E. & Martin, R. Combined experimental and theoretical study on the reductive cleavage of inert C–O bonds with silanes: ruling out a classical Ni(0)/Ni(II) catalytic couple and evidence for Ni(I) intermediates. *J. Am. Chem. Soc.* **135**, 1997–2009 (2013).

Acknowledgements

We thank the financial support from the National Innovation of Science and Technology-2030 (Program of Brain Science and Brain-Inspired Intelligence Technology) Grant of China (2021ZD0204004), the Major Projects for Shanghai Zhangjiang National Independent Innovation of China (ZJ2021-ZD-007), and the grants (WF540162618, AF1700037, WF220217002, WH101117001) from Shanghai Jiao Tong University.

Author contributions

H.L. and R.X.X. contributed equally to this work. H.L. planned, conducted, analyzed and summarized the experiments. R.X.X. established MC38 xenograft model and performed the in vivo antitumor activity assay. C.Y.S., Z.L.S. and H.W.L. participate in the experiments or discussions. H.L. and C.Y.S. wrote the manuscript with feedback from all authors. A.Z. supervised the research. All authors approved the paper.

Competing interests

The authors declare no competing interests.

Additional information

Supplementary information The online version contains supplementary material available at <https://doi.org/10.1038/s42004-022-00694-4>.

Correspondence and requests for materials should be addressed to Ao Zhang.

Peer review information *Communications Chemistry* thanks the anonymous reviewers for their contribution to the peer review of this work. Peer reviewer reports are available.

Reprints and permission information is available at <http://www.nature.com/reprints>

Publisher's note Springer Nature remains neutral with regard to jurisdictional claims in published maps and institutional affiliations.



Open Access This article is licensed under a Creative Commons Attribution 4.0 International License, which permits use, sharing, adaptation, distribution and reproduction in any medium or format, as long as you give appropriate credit to the original author(s) and the source, provide a link to the Creative Commons license, and indicate if changes were made. The images or other third party material in this article are included in the article's Creative Commons license, unless indicated otherwise in a credit line to the material. If material is not included in the article's Creative Commons license and your intended use is not permitted by statutory regulation or exceeds the permitted use, you will need to obtain permission directly from the copyright holder. To view a copy of this license, visit <http://creativecommons.org/licenses/by/4.0/>.

© The Author(s) 2022